Field trip guide

Active faults of the Central Andes along the border of the Principal Cordillera (~32°)

October 7, 2024

Luisa Pinto
Departamento de Geología, Universidad de Chile, Plaza Ercilla #803, Santiago Centro, Santiago, Chile,
lpinto@uchile.cl

Abstract: *This guide presents an itinerary to investigate the active faults on the western border of the Andes, which can be done in around three hours of fieldwork along main roads in the Piedmont. A total of 3 field stops are organized in a main structural system, Cariño Botado Fault, in the wester border of the Principal Cordillera (32°30'S-33°S). The proposed sectors exhibit clear structural, morphotectonic, stratigraphic, and sedimentary features supporting active faulting in the Andean Mountain orogen. According to the recent bibliography, the geological features mentioned in this guide are widely documented and contextualized. We studied these faults using different methods. We incorporated analysis of alluvial and fluvial stratigraphy, fluvial terraces, pediments, morphometric indicators, in-field fault descriptions, knickpoints, remote sensing, mapping geology, thermoluminescence OSL, and U-Pb ICPMS dating. Using this information, we could define and understand the Cariño Botado Fault System and calculate here for the first-time tectonic rates. The Cariño Botado Fault System comprises at least two faults and two lineaments. From west to east, they are the San Francisco Fault, the main fault of the Cariño Botado fault system 500 m to the east, and two additional lineaments located further east. These eastern lineaments show morphometric evidence of tectonic activity, which needs more studies. To the north of the area is a block with a horizontal surface: La Mesilla Hill. It is a fluvial terrace about 100 m over the riverbed of the San Francisco Creek that was uplifted by the Cariño Botado Fault System.*

Keywords: Active faults · Principal Cordillera · Field trip guide · Central Andes · Chile

Highlights

- Tectonic geomorphology of a west-vergent thrust at a flat slab of the Andes.
- Studies fault exposures, uplifted terraces, and tilted alluvial fan deposits.
- Fault activity dated by OSL and U-Pb applied to geomorphic markers.
- Space-time similarities between the San Ramón and Cariño Botado faults.
- Cariño Botado faults suggest a possible seismic hazard of up to Mw 7.5.
- To the north of the area is a block with a horizontal surface: La Mesilla Hill. It is a fluvial terrace about 100 m over the riverbed of the San Francisco Creek that was uplifted by the Cariño Botado Fault System.

Links of interest:

https://geologia.uchile.cl/noticias/210845/investigadores-describen-falla-geologica-en-region-de-valparaiso

Active thrust tectonics along the western slope of the Central Andes southernmost Pampean flat-slab segment (~33°S, Chile): The Cariño Botado fault system

1. Introduction

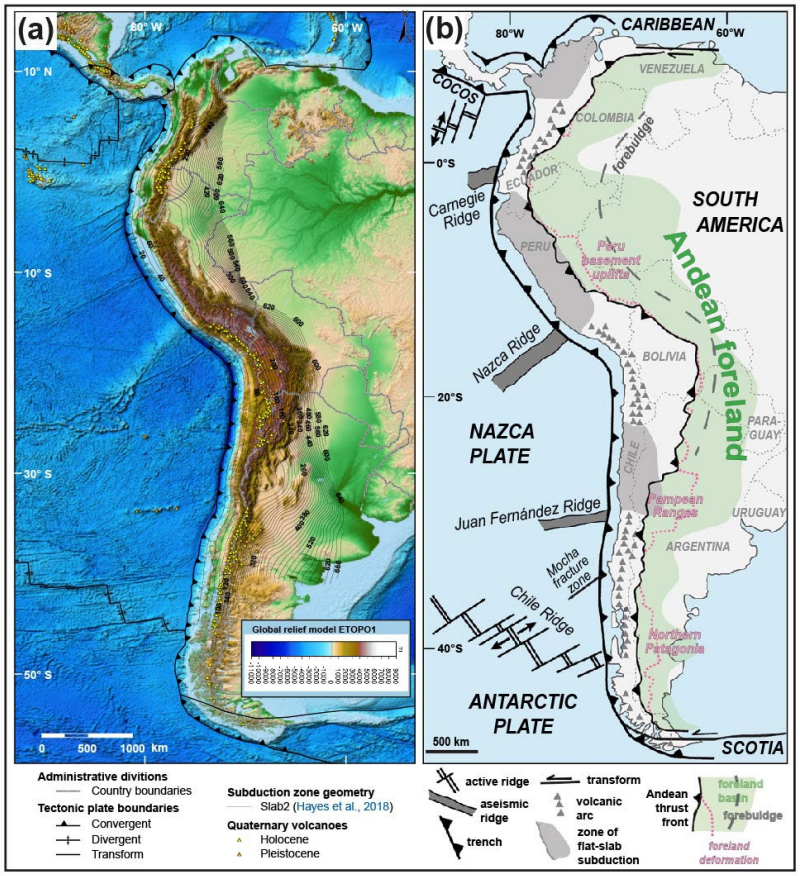

Fig. 1 (a) Shaded topography of western South America (San Juan et al., under revision), and **(b)** Tectonic map (taken from Horton et al., 2022), showing plate boundaries, volcanic arc, zones of flat-slab subduction (grey areas), and selected basin segments (black labels). The topographic front of the Andean fold-thrust belt (black barbed line) and foreland deformation front (pink line) are indicated.

The **Andes of South America** are a classic example of a non-collisional orogen, related to subduction and developed mainly during the Cenozoic by the convergence of the South American and Nazca Plates (**Fig. 1**) (e.g., Jordan et al., 1983a; Gutscher et al., 2000; Charrier et al., 2007). This orogen presents a latitudinal morpho-structural segmentation, reflecting variations in subduction angle, convergence rate, basement composition, thickness, climate, and internal structures of the South American Plate, and the presence of oceanic ridges within the Nazca Plate, such as the **Juan Fernández Ridge** (e.g., Jordan et al., 1983a, b; Pardo-Casas and Molnar, 1987; Gutscher et al., 2000; Sobolev and Babeyko, 2005; Charrier et al., 2007; Manea et al., 2012; Jara and Charrier, 2014; Mescua et al., 2016; Martinod et al., 2020). In the **Pampean flat-slab segment**, located between 27° and 33°S, the Nazca Plate subducts towards the east, at an angle of 5-10° (i.e., approximately "flat"; Barazangi and Isacks, 1976) under the South American Plate. However, to the south of 33°S in a **normal segment**, it subducts at an angle of ~30° (e.g., Gutscher et al., 2000; Anderson et al., 2007; **Fig. 2**). The upper crust of the upper plate along these subduction segments shows evidence of long-term contractional deformation starting in the early Miocene (e.g., Cristallini and Ramos, 2000; Charrier et al., 2007; Armijo et al., 2010; Farías et al., 2010; Jara and Charrier, 2014; Lossada et al., 2017; Rodríguez et al., 2018). The styles and patterns of morpho-structural domains to the north (i.e., flat subduction segment) and south (i.e., normal subduction segment) of ~33°S depend on the tectonic configuration (**Fig. 2**). The Principal Cordillera is one of the morpho-structural features that extends continuously through both segments (**Fig. 2**; Jordan et al., 1983b; Gutscher et al., 2000).

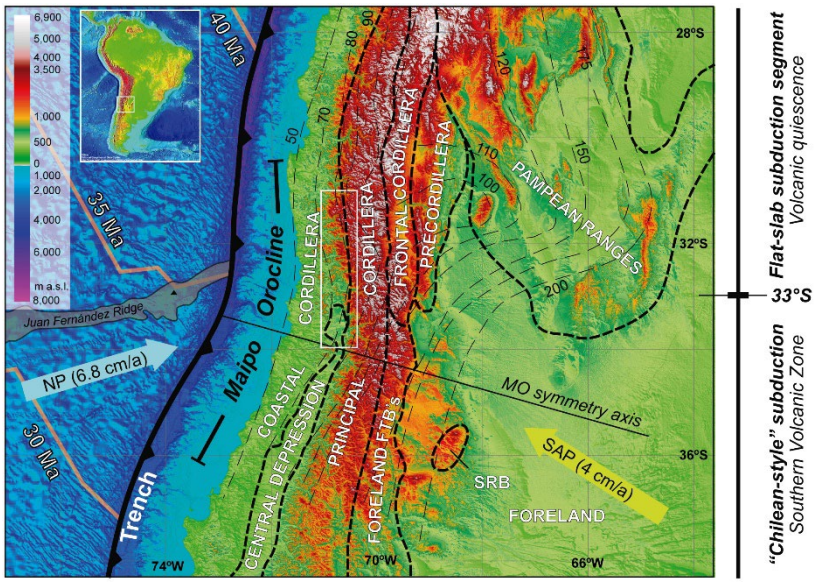

Fig. 2. Global geodynamic and tectonic framework with the main morpho-structural features of the study region (modified from Herrera et al., 2017; Estay et al., 2023). The white box indicates the area of **Fig. 3**. MO, Maipo Orocline; NP, Nazca Plate; SAP, South American Plate; SRB, San Rafael Block. The curves show the depth of the Benioff plane in km (after Anderson et al., 2007). The convergence velocity of plates in the flat-slab segment is indicated (DeMets et al., 2010; Vigny et al., 2009). Note the location of the Juan Fernandez Ridge subducting under the study region.

Between 32.5° and 33°S, the western edge of the Principal Cordillera is defined by a topographic rupture coinciding with an old west-vergent reverse fault system, the **Pocuro Structural System** (e.g., Rivano, 1996; Rivano et al., 1993; Pérez et al., 2023; Millanao et al., 2023), which limits the Principal Cordillera with the Los Andes-San Felipe Depression (**Fig. 3**). Non-deformed intrusives (dykes, sills, stocks) within this fault zone indicate that it was active at least since the early Miocene (Gana and Wall, 1997; Padilla and Vergara, 1985). The main fault trace of the Pocuro Structural System has an altered and brecciated zone of 0.5-2 km wide (Rivano et al., 1993; Rivano, 1996); in addition, minor faults can be recognized up to ~4 km east of this zone (Urrejola-Sanhueza, 2022). This structural system is traditionally considered the western edge of the Principal Cordillera. Within this structural system is the **Quaternary Cariño Botado Fault** (**Fig. 3**), part of this field trip.

South of 33°S, the western edge of the Principal Cordillera, the West Andean Thrust front, is defined by its border with the Central Depression (**Fig. 3**) (e.g., Charrier et al., 2002, 2007; Armijo et al., 2010; Farías et al., 2010). Santiago city faces the frontal relief of the Andes associated with the emergence of the west Andean thrust along a segment called the San Ramon fault (SRF; **Figs. 3 and 4**). Uplift of the Cordillera Principal by the slip of the SRF during the past millions of years has produced the dramatic escarpment that rises to San Ramon peak and the Farellones Plateau, 2.7 km and 2 km, respectively, above the city. Several studies have shown that the San Ramón Fault belongs to an along-lived major fault zone, which has probably been active since the Oligocene (e.g., Charrier et al., 2002; Armijo et al., 2010; Farías et al., 2010; Muñoz-Sáez et al., 2014 and references cited therein). The surface trace of the fault is clearly expressed by a semicontinuous scarp that extends north to south for at least 35–40 km from Río Mapocho to the south of Río Maipo (**Fig. 4**) (Armijo et al., 2010).

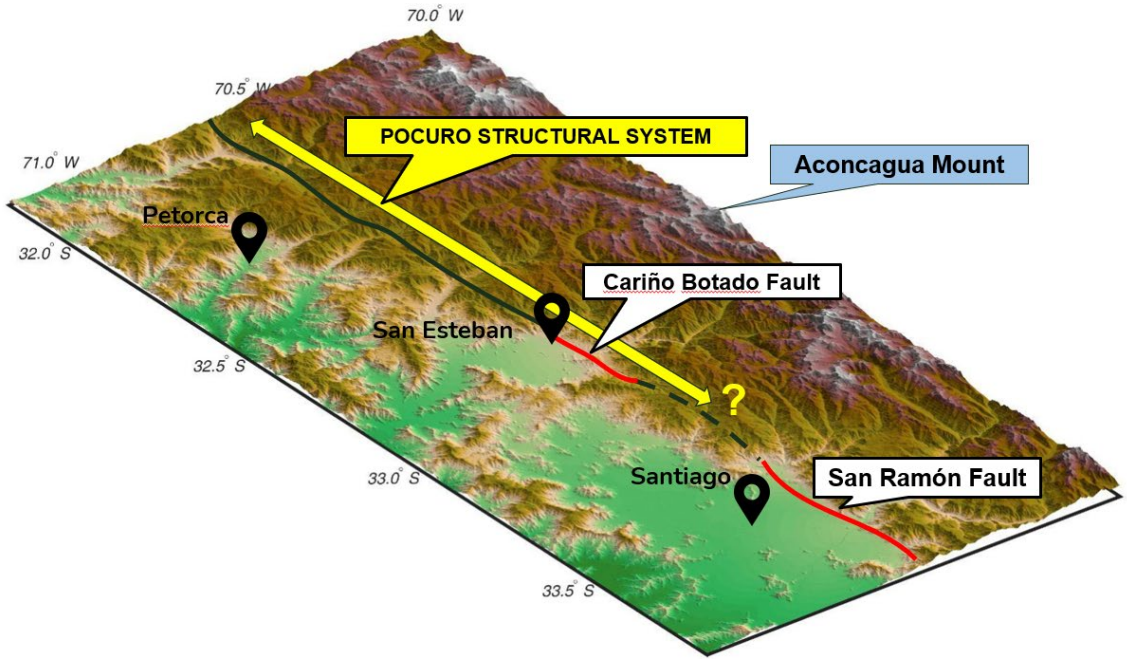

Fig. 3 DEM showing the connection between the traces of the Cariño Botado Fault and the San Ramón Fault trace (~33°30'S). Image modified from Estay et al. (2018).

The geometric and temporal evolution of the Cariño Botado and San Ramón Fault (**Fig. 3**) and their relationship in the region have been under-studied, despite their relevance regarding seismic risk assessment (Easton et al., 2018; Hussain et al., 2020; Inzulza et al., 2021; 2022; Ammirati et al., 2022). Only during the last decade, a series of works developed on the Cariño Botado Fault has partially revealed its Quaternary activity (Troncoso, 2014; Medina, 2018; Estay, 2019; Figueroa et al., 2021; Taucare et al., 2022; Estay et al., 2023), but critical parameters for seismic hazard characterization, such as the age and slip rates of recent faulting, remain unknown.

2. Relationship between intraplate earthquakes of the western border of the Central Andes

The largest earthquakes on Earth (moment magnitude, M_w 8–9; Hanks and Kanamori, 1979) are generated by fault rupture at major plate boundaries, generally in subduction zones, producing regionally widespread destruction. However, rupture of secondary fault zones associated with internal deformation of plates and located closer to populated areas can produce intense local destruction in major cities, even if those events are of moderate to large magnitude (M_w ~ 7) (Dolan et al., 1995; Rubin et al., 1998; Bilham, 2009; Ritz et al., 2012). An example is the catastrophic 1995 M_w 6.8 Kobe earthquake in Japan, which killed more than 6000 people (Kanamori, 1995). Tragically, the hazard associated with those killer events has often been correctly assessed after their occurrence. The same problem applies to important secondary thrust faults associated with the generation of frontal relief of mountain belts, especially around active growing orogens like Tibet and the Andes Mountains of South America. Again, the importance of the potential hazard of the Long Men Shan thrust, located at the eastern flank of Tibet, was dismissed (Clark et al., 2005) prior to its nearly complete rupture in 2008 that produced the M_w 7.9 Wenchuan earthquake (Xu et al., 2009).

The Chilean subduction margin of South America has produced some of the largest earthquakes worldwide (Cifuentes and Silver, 1989; Brooks et al., 2011). However, the neighboring topographic relief of the Andean orogen is not directly associated with subduction processes but was created by secondary frontal thrust systems at major Andean ranges (Armijo et al., 2010; Brooks et al., 2011). Identifying the seismic potential of such thrusts is difficult because large earthquakes there are much less frequent than on the main plate boundary (typically 100× less). While the potential for large thrust earthquakes along the eastern flank of the Andes is now recognized (Brooks et al., 2011), very few events have been accurately recorded historically, and only some moderate-magnitude events have been recorded instrumentally (Alvarado and Beck, 2006) or in paleoseismological trenches, such as the M_s ~ 7 earthquake that destroyed Mendoza, Argentina, in 1861 (Salomon et al., 2013). On the opposite flank of the orogen, the prominent west Andean thrust (**Fig. 4**), which has geometry and vergence similar to those of the relatively close subduction plate interface, was identified only recently, and the problem of its seismic potential is starting to be considered (Armijo et al., 2010; Pérez et al., 2013).

Recent activity in the **San Ramón Fault** (**Figs. 3 and 4**) indicates that it has west-vergent reverse kinematics and can generate earthquakes (M_w ~ 7.2-7.5) with surface ruptures and recurrence intervals on the order of thousands of years, based on tectonic geomorphology, and paleo-seismological and seismological studies (Vargas et al., 2014; Ammirati et al., 2019, 2022). The paleoseismological study by Vargas et al. (2014) revealed evidence that the large intraplate earthquakes occurred since 17–19 ky, demonstrating active tectonic growth of the western flank of the Andes and implying increased seismic risk for the city of Santiago.

Evidence of **Holocene tectonic activity has also been shown for the Cariño Botado Fault**, with potential seismicity of up to Mw 7.5, similar to the San Ramón Fault. In this field trip, we will examine the similarities between these two structural systems on the western edge of the Principal Cordillera.

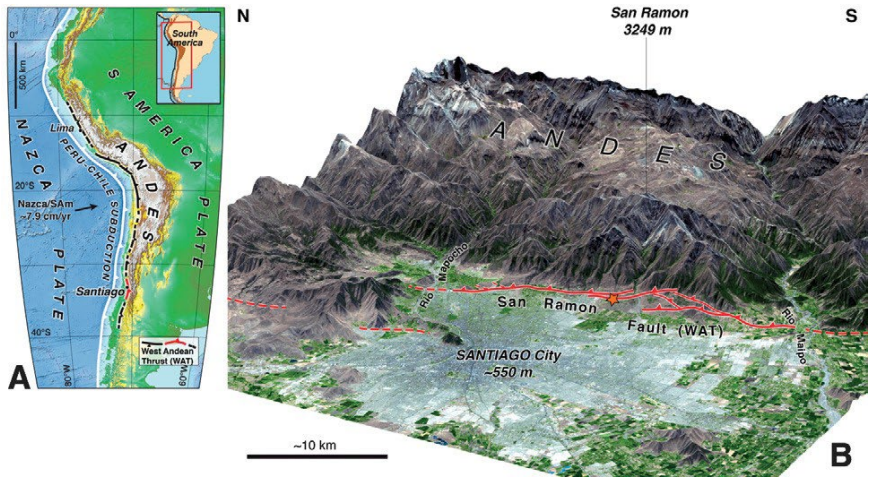

Fig. 4. Extent of the west Andean thrust (WAT; Armijo et al., 2010), South America (SAm). **A:** The WAT is the main active continental-scale fault system at the western foot of the An- des, breaking the west margin of the continent ~200 km eastward from the trench. The Santiago segment of the WAT is in red, and the other parts are in black (dashed where less certain). **B:** Three-dimensional view of Santiago conurbation (more than six million inhabitants) and fault scarps at the piedmont of the abrupt Andean Mountain front [SPOT satellite image draped over 30 m digital elevation model, courtesy of Centre National d'Etudes Spatiales]. The orange star shows the location of the paleoseismological trench (from Vargas et al., 2014).

3. Field Guide: Cariño Botado Fault System (CBF)

For this first day in the field, we will visit **3 outcrops of the Cariño Botado Fault System (CBF)**. The following will present the route with map figures, profiles, and photographs to help you better understand the information presented during the visit.

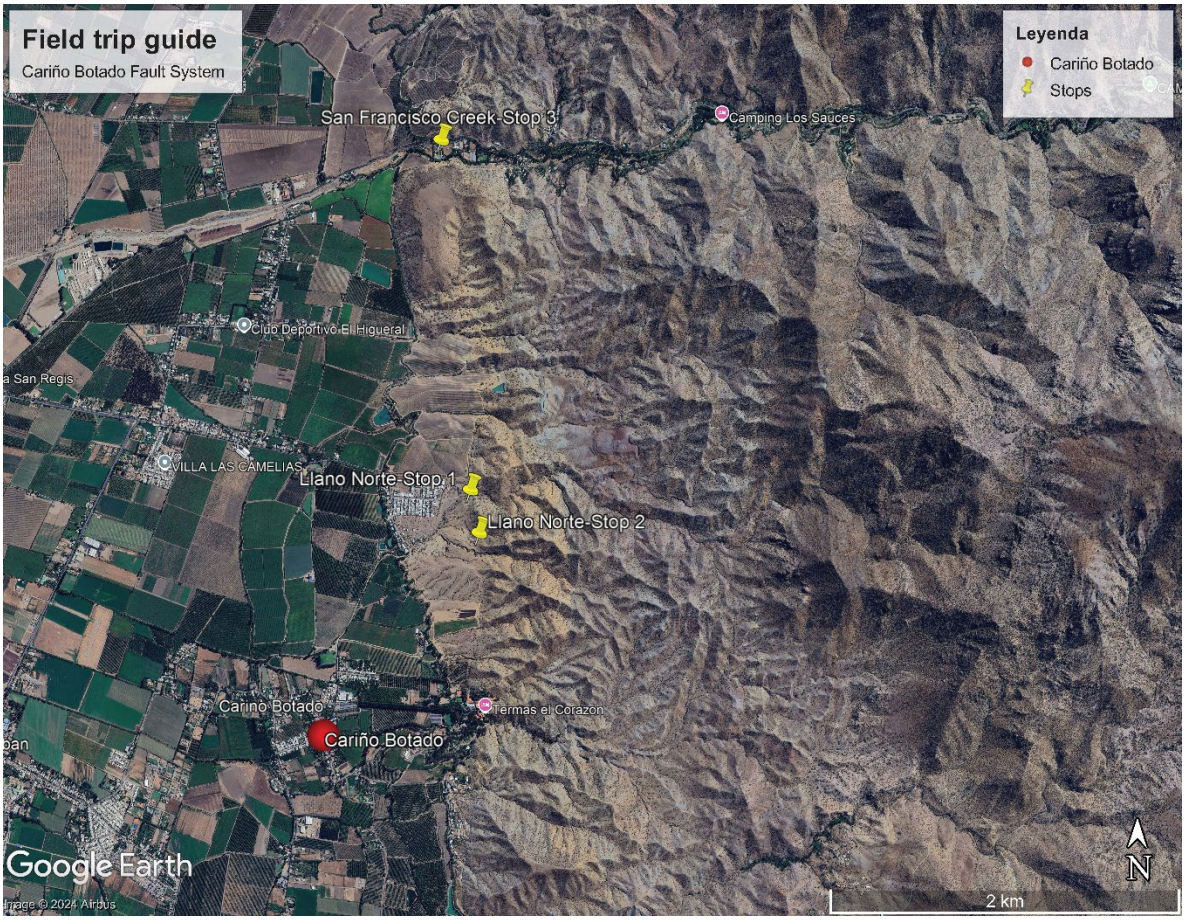

Fig. 5. Google Earth image showing the localities and stops of the field trip to the Cariño Botado Fault System (CBF).

Departure and route

The field trip begins at **Termas El Corazón**, where we are staying, located directly over the main trace of the **Cariño Botado Fault System (CBF)**. From here, we will head to the main route of San Esteban, passing by the town square to observe, on the way looking east, a magnificent view of the Pocuro Fault Zone with its low, colorful hills (**Fig. 5**). From this viewpoint, you will also see La Mesilla Hill (**Fig. 5**), a plateau with fluvial deposits from the San Francisco stream that were uplifted 100 m above the streambed. These fluvial deposits have a maximum age of ~900 ka (Estay et al., 2023). Note also that our route will be at an elevation of ~920 m a.s.l., which contrasts with the edge of the mountain range that quickly reaches 1020 m a.s.l. We will then take a curve to head straight toward the CBF in the Llano Norte area, where we will be welcomed by the resident, Carmen Quiroga, who lives right in the fault zone ('abuelita del Cerro').

Landscape, climate, flora and fauna

In this field trip, we visit the western border of the Principal Cordillera between 32°-33°S, which features a varied landscape dominated by the Andes Mountains' western slopes. This area is characterized by steep terrain, deep valleys, and occasional river gorges. The region falls within a Mediterranean climate zone, with hot, dry summers and cool, wet winters, creating conditions for a unique mix of ecosystems. The flora primarily comprises sclerophyllous forests and shrublands adapted to withstand long dry periods. Key species include the **quillay**, **peumo**, **boldo**, and **lithraea**. These forests are often accompanied by diverse matorral communities, which include shrubs like **chilca** and **espino**, adapted to the dry, rocky soils. The fauna in this region is equally distinctive, with notable species such as the **guanaco**, **puma**, and the **Andean fox**. The birdlife includes the **Andean condor**, **black-chested buzzard-eagle**, and **burrowing parrot**. Reptiles, including various species of **Liolaemus lizards** and amphibians like the **four-eyed frog**, further contribute to the region's biodiversity. The combination of diverse topography and Mediterranean climate supports ecosystems with high levels of endemism and ecological significance (Armesto et al., 2007).

Sources: Espino on the top: https://www.nublenaturaleza.cl/articulos/flora/arboles/espino; Andean condor below: https://www.13.cl/c/programas/espacio-13c/conoce-al-majestuoso-condor-andino-cada-7-de-julio-celebra-su-dia

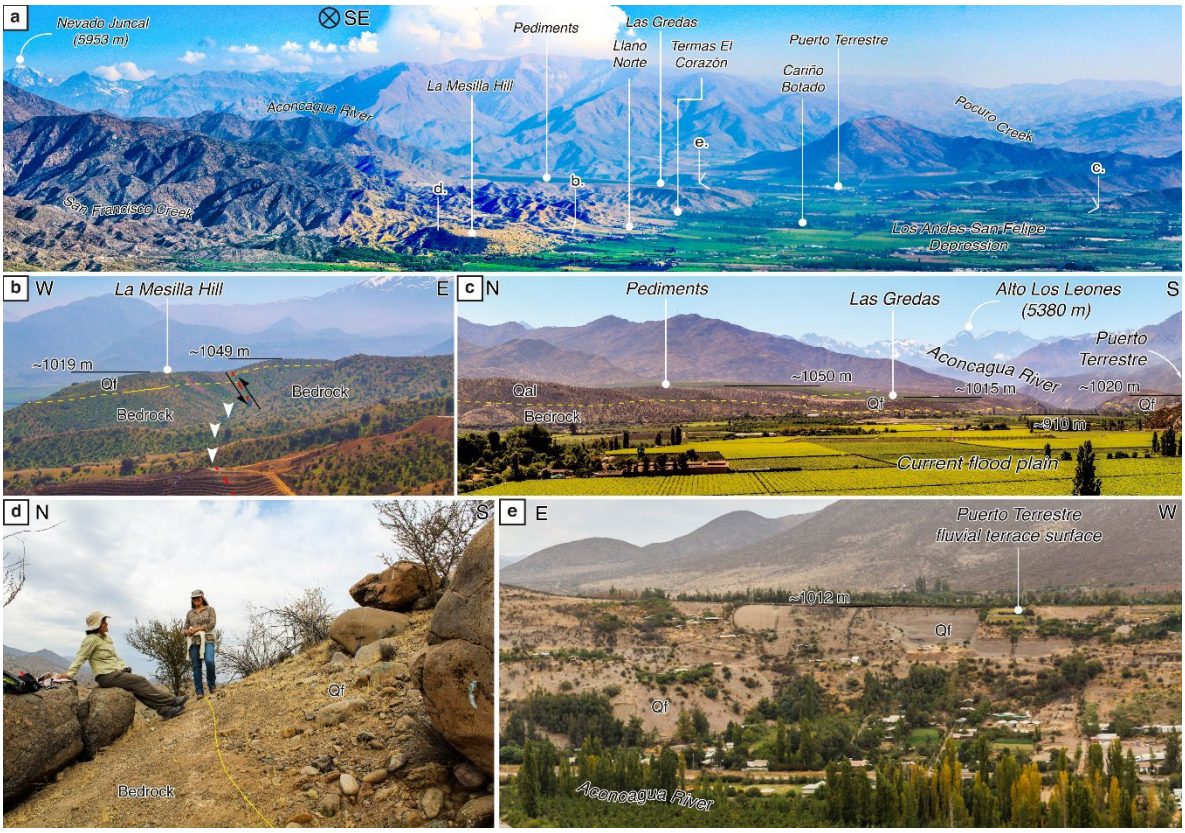

Fig. 6. Field photos of the study area and primary geomorphological markers. **(a)** General overview of the mountain front and foothills, showing localities, the main geographical features, and the locations of the viewpoints of **Figs. 6b, 6c, 6d and 6e**. **(b)** Profile view of the strath terrace of La Mesilla Hill; note the vertical offset of the paleo-river surface (~30 m) due to the movement of the CBF's main fault indicated in the photograph. **(c)** Relationship between alluvial pediments, the Las Gredas fluvial terraces, and the current Aconcagua River floodplain. **(d)** Contact between a bedrock strath and the oldest fluvial deposits (Qf, **Fig. 7**) near the summit of La Mesilla Hill. **(e)** Fluvial terrace of Puerto Terrestre; the oldest fluvial deposits (Qf, **Fig. 7**) are exposed in quarries. Surface and hill heights correspond to meters above sea level.

Stop 1: Llano Norte-north

- Feature: CBF's main trace, UTM: 355031.00 m E / 6371430.65 m S
- Directions: Routes E-755 to E-761, Llano Norte – north
- Description: Panoramic view of the mountain front, western edge of the Chilean Principal Cordillera. At this stop, we are standing directly on the **Pocuro Structural System**. Also, note that we are standing on the youngest alluvial fan recognized in the area (**~2.5 ka, Qal2**, **Fig. 7**; Estay et al., 2023). The main slope break is marked by the main trace of the CBF (**Fig. 8**). This west-verging reverse fault has a 40°E dip, producing a **scarp of ~3.2 m and a slip-fault of ~4.9 m** (**Figs. 8 and 9**; Estay et al., 2023). There is another fault outcrop point just north of the creek, next to the house of Mrs. Carmen Quiroga (**Fig. 10d**). The slope break in the morphology is notable, showing yellowish altered rocks from the **Abanico Formation** (~34 Ma), overriding the older alluvial deposits in this area (**~8.7 ka, Qal1**, **Fig. 7**; Estay et al., 2023). This is the best outcrop of the main fault of the CBF (**Fig. 8**) and where samples for dating were obtained. We can go down to the creek to observe the outcrops and sedimentary facies of the fans up close.

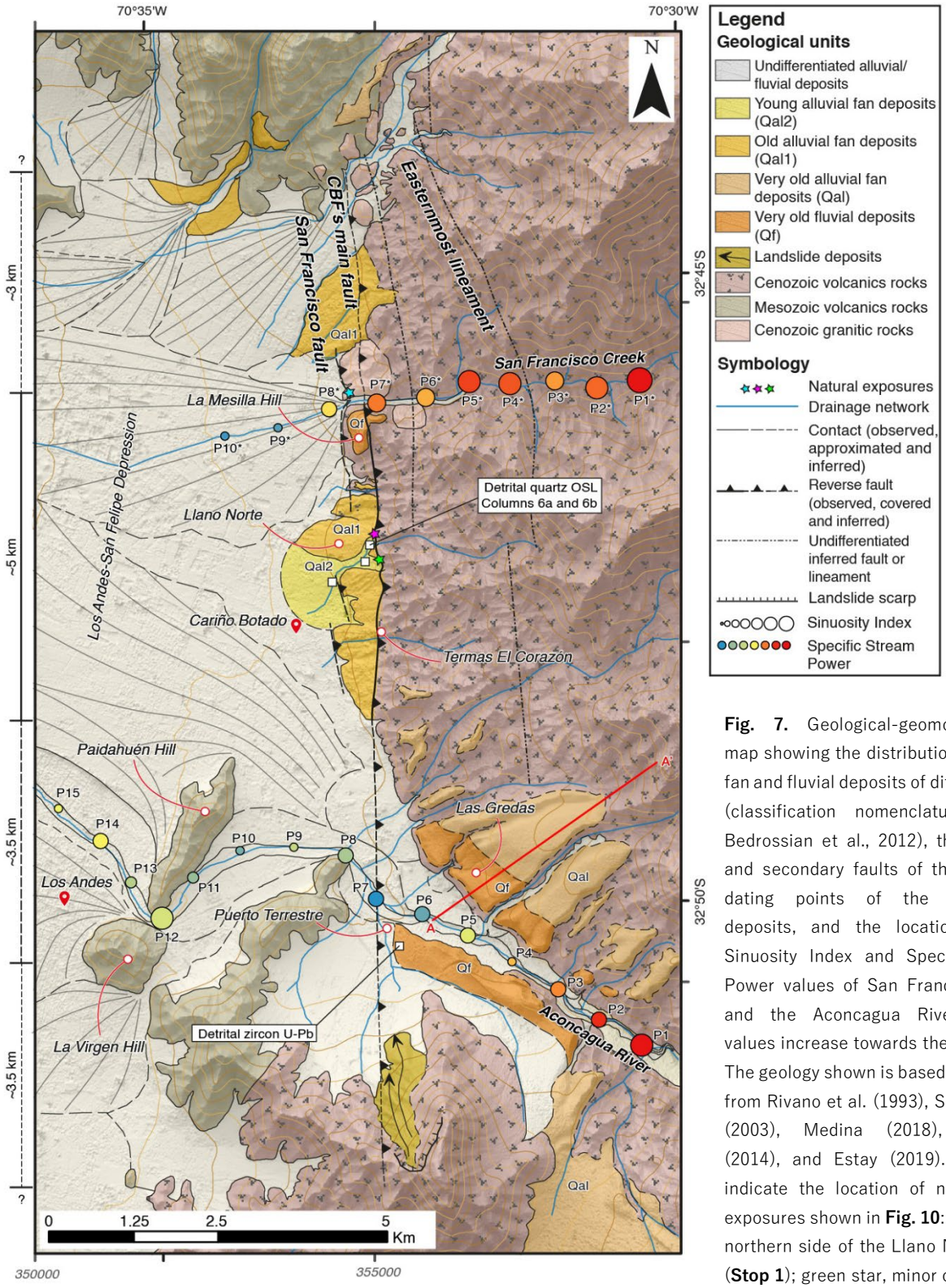

Fig. 7. Geological-geomorphological map showing the distribution of alluvial fan and fluvial deposits of different ages (classification nomenclature follows Bedrossian et al., 2012), the principal and secondary faults of the CBF, the dating points of the Quaternary deposits, and the locations of the Sinuosity Index and Specific Stream Power values of San Francisco Creek and the Aconcagua River (legend: values increase towards the right side). The geology shown is based on the data from Rivano et al. (1993), Sernageomin (2003), Medina (2018), Troncoso (2014), and Estay (2019). The stars indicate the location of natural fault exposures shown in **Fig. 10**: purple star, northern side of the Llano Norte Creek (**Stop 1**); green star, minor creek south to the Llano Norte Creek (**Stop 2**); light blue star, San Francisco fault (**Stop 3**). Topographic base: 4 m/px digital elevation model (modified from Estay et al., 2023).

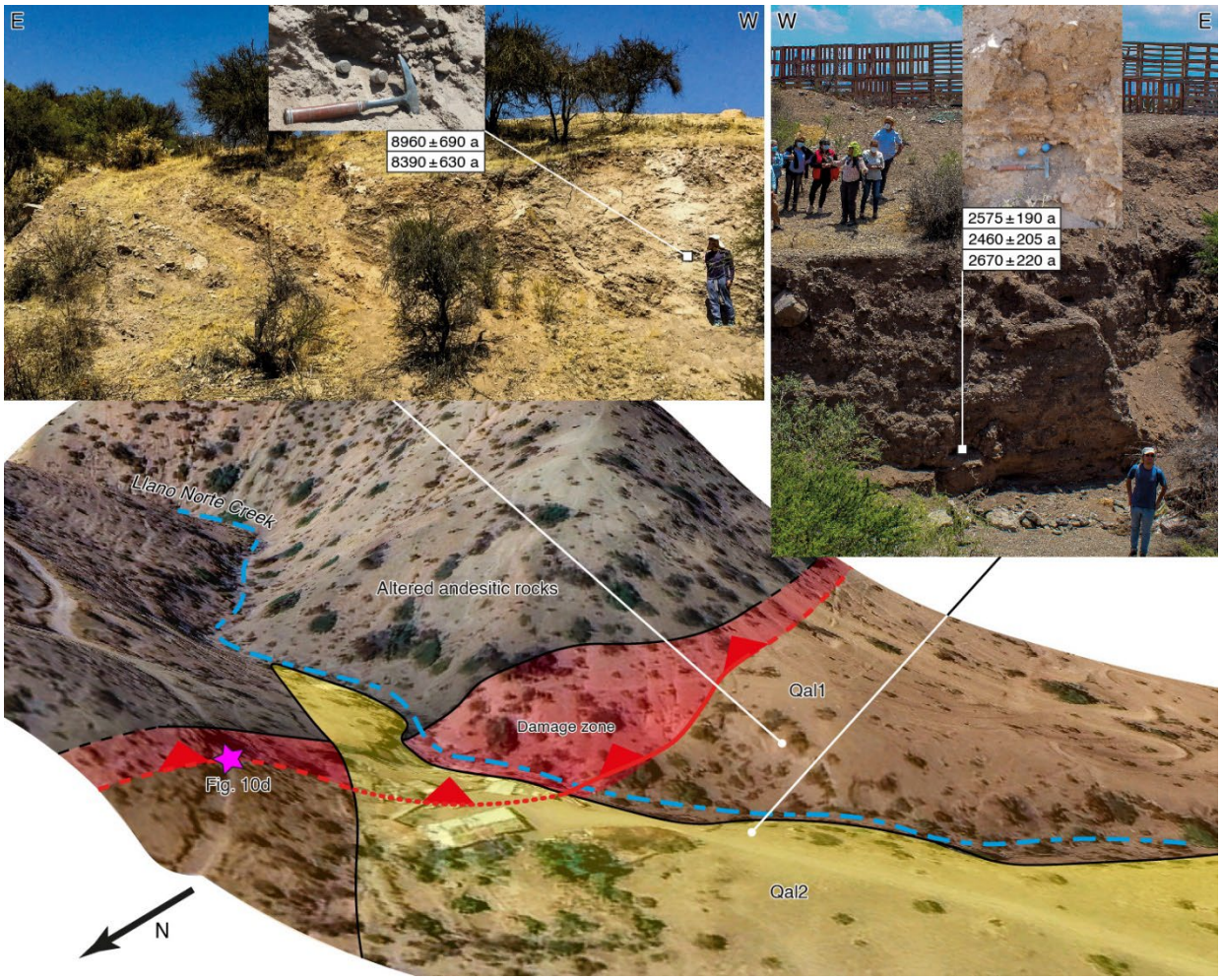

Fig. 8. 3D sketch with a SE view of the CBF's main fault and alluvial fan deposits (Qal1 and Qal2) in the Llano Norte sector (see location in **Fig. 6**) (modified from Estay et al., 2023). The photographs show the geometric relationship of the old (Qal1) and young (Qal2) alluvial fan deposits around the CBF's main fault. Field photos with the location of the OSL-dated samples are indicated. Image © 2023 Maxar Technologies from Google EarthTM.

Stop 2: Llano norte-south

- Feature: CBF's main trace, UTM: 355091.56 m E / 6371168.87 m S
- Directions: Routes E-755 to E-761, Llano Norte – south
- Description: Be careful while walking, as the material is loose. In this second outcrop of the main trace of the CBF, we can observe the contact between the Abanico Formation (Oligocene) and the older Quaternary alluvial deposits (Qal1, **Fig. 7**), marked by a fault gouge (**Fig. 10c**). At this stop, we can also clearly see the significant alteration of the Abanico Formation rocks with Fe and Mn oxides, which give the rocks a yellowish hue. Additionally, if we observe the more incised outcrops, we can see the layers of the alluvial fan dipping at ~40°W (**Figs. 10c and 10e**). This strata dip is pronounced in this area just above the fault, but moving westward, the layers have a normal inclination for alluvial deposits (~5°W) (**Fig. 8**). We have interpreted this greater dip near the fault as drag folding (**Fig. 9**; Estay et al., 2023).

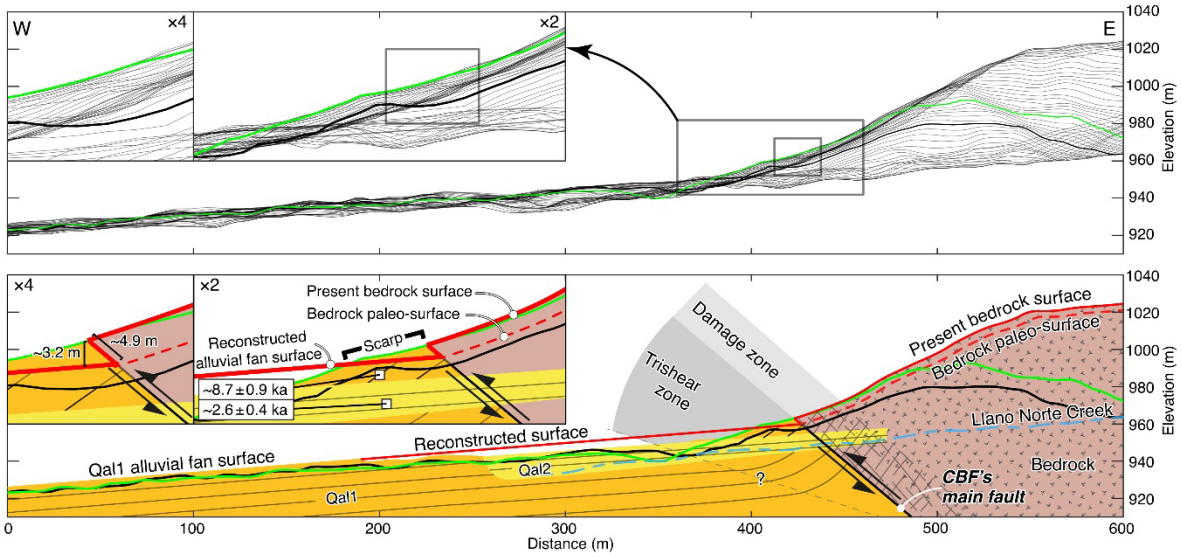

Fig. 9. Swath profile and geological interpretation of deformation associated with the CBF´s main fault in the Llano Norte sector (**Fig. 7**) (from Estay et al., 2023). From this profile analysis, a vertical dislocation of ~3.2 m was estimated between the reconstructed Llano Norte alluvial fan surface (Qal1) with the present bedrock surface to the east of CBF's main fault. The green line corresponds to the central axis of the swath profile (baseline), the black line highlights the profile that passes just over the outcrop of Qal1 tilted sediments, the red line corresponds to the interpreted approximate isochronous that connects preserved Qal1 alluvial fan surface and present bedrock surface, and the segmented red line is the interpreted bedrock paleo-surface.

Stop 3: San Francisco Creek

- Feature: San Francisco Fault, UTM: 354799.84 m E / 6373574.20 m S
- Directions: Route E-763, San Francisco Creek
- Description: In this outcrop, we can observe the **secondary fault** of the CBF, called the San Francisco Fault (**Figs. 10a-b**), located about **500 m west of the main fault**. We can appreciate how the **altered rocks of the Abanico Formation thrust the quaternary deposits**. It is also a **west-vergent, reverse fault, 40° east-dipping, with a vertical offset of around 2.3 m and an apparent slip of about 3.6 m**. Looking to the south, there is a **strath terrace covered by a thin layer of fluvial deposits** (**Fig. 6d**). This strath terrace is deformed by the main fault of the CBF, producing an **offset of ~30 m**. We propose that the San Francisco Fault has caused the uplift of this strath terrace by around **100 m**, which explains its current position above the riverbed of San Francisco Creek. We also used **U-Pb ICPMS to date detrital zircons from terrace fluvial deposits** correlated with those of the La Mesilla Hill, which young zircons suggesting a Holocene tectonic activity **started at ~0.9 Ma ago**, considering that the CBF uplifted the La Mesilla Hill block. Besides, variations in the Specific Stream Power (SSP) in the San Francisco Creek are related to faults or potential faults recognized in this creek (**Fig. 7**); in the Aconcagua River, the SSP is controlled mainly by the CBF's main Fault (**Fig. 7**), with a **dominance of erosive processes upstream** (east of the main fault) **and dominance of deposition processes** to the west of it. We propose a **tectonic control** over the Specific Stream Power, supported by the **distribution of fluvial terraces located only east of the main fault** of the system (**Fig. 7**). This evidence is crucial because it indicates an **uplift of ~100-130 m** for the **Principal Cordillera** in this area, maybe **since 0.9 Ma**, explained by the activity of the CBF with an incision rate of ~0.1 mm/yr that can be interpreted as the uplift rate.

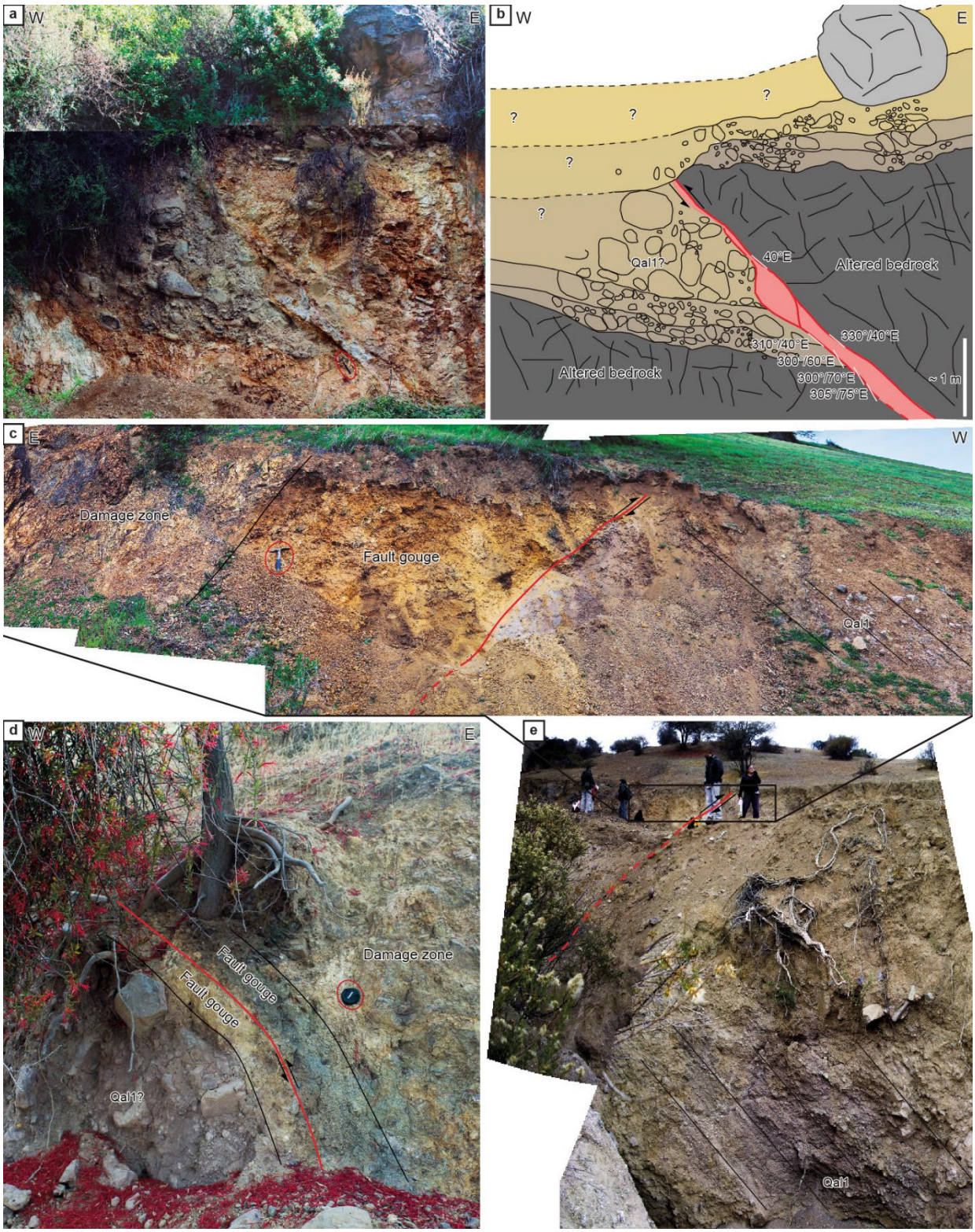

Fig. 10. Photographs and diagram of natural fault exposures along the CBF on the eastern edge of the Los Andes-San Felipe Depression (modified from Estay et al., 2023). **(a)** and **(b)** natural exposure and paleoseismological scheme of the west secondary fault identified in the San Francisco Creek (see location in **Fig. 7**, light blue star). Structural strike/dip data from Medina (2018). **(c)**, **(d)**, and **(e)** Natural exposures of the CBF's main fault in the vicinity of Llano Norte locality, showing different dimensions of fault gouge and its relationship with the damaged zone and tilted Qal1 alluvial fan sediments (see location in **Fig. 7**: 10c green star, and 10d purple star).

Photograph: Jipria Herrera Ahumada.

The Cariño Botado Legend

These were the days when the Army of the Andes was preparing to liberate Chile once and for all. Villa Santa Rosa was the center of information. Spies and muleteers brought news of the maneuvers being carried out on the other side of the Cordillera for the entry of the army columns through the fertile valley of the Aconcagua.

[The Cariño sector was always a place of passage; it was close to the road that led to Argentina, and also, through the plains sector, they traveled to San Francisco, where there is a mountain pass to Argentina. In addition, muleteers used to go a lot to Cuyo in Argentina, bringing animals back and forth, as well as cattle thieves who went to steal livestock, so there were inns for travelers to rest, there were plenty of houses where they sold chicha, chacoli, punch, as well as musicians playing guitars.]

The few inhabitants of a place very close to Los Andes, once a stronghold of Michimalonco, had heard from muleteers that part of the army would be passing very close to their village, and as they were a very affectionate people and had a lot of livestock, fruit and vegetables and good drink in their area, they decided to prepare a welcome for the soldiers by giving them 'un cariñito' ('a little treat'), as they used to say when they offered food and drink to their visitors.

As soon as they were informed that the libertarian troops were near, all the inhabitants of the village that are now known as 'Cariño Botado' began preparations with great enthusiasm, using their livestock, vegetables, and rich grape juice to make a 'cariñito' ('a little treat) for the brave patriots. When everything was ready to offer the banquet, a messenger brought the sad news that, by order of General José de San Martín, the column of Las Heras had to continue its march quickly to join the rest of the Liberation Army in Curimón and continue from there to Chacabuco.

The caring villagers were very saddened that all the preparations to receive the brave soldiers were ruined and their 'affection – 'cariño' – was thrown away'. Since then, this picturesque place in the commune of San Esteban, only a few kilometers from Los Andes, took the name of 'Cariño Botado', still preserving the tranquility of the mountain people.

The legend of this attractive Andean corner awakens the interest of the visitors who come to Cariño Botado to find the toponymy and the aroma of history that its surroundings offer.

Carlos Tapia Canelo (1944)

4. References

Alvarado, P., Beck, S., 2006. Source characterization of the San Juan (Argentina) crustal earthquakes of 15 January 1944 (Mw 7.0) and 11 June 1952 (Mw 6.8). Earth Planet. Sci. Lett. 243, 615–631, doi:10.1016/j.epsl.2006.01.015.

Ammirati, J.-B., Vargas, G., Rebolledo, S., Abrahami, R., Potin, B., Leyton, F., Ruiz, S., 2019. The Crustal Seismicity of the Western Andean Thrust (Central Chile, 33°–34°S): Implications for Regional Tectonics and Seismic Hazard in the Santiago Area. Bull. Seismol. Soc. Am. 109(5), 1985–1999.

Ammirati, J.-B., Villaseñor, A., Chevrot, S., Easton, G., Lehujeur, M., Ruiz, S., Flores, M.C., 2022. Automated earthquake detection and local travel time tomography in the South-Central Andes (32–35°S): Implications for regional tectonics. J. Geophys. Res. Solid Earth 127, e2022JB024097. https://doi.org/10.1029/2022JB024097.

Anderson, M., Alvarado, P., Zandt, G., Beck, S., 2007. Geometry and brittle deformation of the subducting Nazca Plate, Central Chile and Argentina. Geophys. J. Int. 171(1), 419–434. ISSN 0956540X. https://doi.org/10.1111/j.1365-246X.2007.03483.x.

Armesto, J.J., Arroyo, M.T.K., Hinojosa-Opazo, L., 2007. Mediterranean-Type Ecosystems in Central Chile and various academic resources on Chilean biodiversity. Central Chile Ecosystems Overview. In: Veblen, T.T., Young, K.R.; Orme, A.R. (Eds.), The physical geography of South America, pp. 184-199. ISBN: 9780195313413. https://repositorio.uchile.cl/handle/2250/120061.

Armijo, R., Rauld, R., Thiele, R., Vargas, G., Campos, J., Lacassin, R., Kausel, E., 2010. The West Andean Thrust, the San Ramón Fault, and the seismic hazard for Santiago, Chile. Tectonics 29, TC2007. https://doi.org/10.1029/2008TC002427.

Barazangi, M., Isacks, B.L., 1976. Spatial distribution of earthquakes and subduction of the Nazca plate beneath South America. Geology 4(11), 686–692. ISSN 0091-7613. https://doi.org/10.1130/0091-7613(1976)4<686:SDOEAS>2.0.CO;2.

Bedrossian, T.L., Roffers, P.D., Hayhurst, C.A., Lancaster, J.T., Short, W.R., McCrea, S., Wanish, B., Thompson, J., Carney, A., Myers, M.A., Utley, S., 2012. Geologic Compilation of Quaternary Surficial Deposits in Southern California. California Geol. Surv. Spec. Rept. 217 (Revised), 21 pp., 25 plates, https://www.conservation.ca.gov/cgs/publications/sr217.

Bilham, R., 2009. The seismic future of cities. Bull. Earthquake Eng. 7, 839–887. doi:10.1007/s10518-009-9147-0.

Brooks, B.A., Bevis, M., Whipple, K. et al., 2011. Orogenic-wedge deformation and potential for great earthquakes in the central Andean backarc. Nat. Geosci. 4, 380–383. https://doi.org/10.1038/ngeo1143.

Charrier, R., Baeza, O., Elgueta, S., Flynn, J., Gans, R., Kay, S., Muñoz, N., Wyss, A., Zurita, E., 2002. Evidence for Cenozoic extensional basin development and tectonic inversion south of the flat-slab segment, southern Central Andes, Chile (33°–36°S). J. South Am. Earth Sci. 15, 117–139.

Charrier, R., Pinto, L., Rodríguez, M.P., 2007. Tectonostratigraphic evolution of the Andean Orogen in Chile, In: Moreno, T., Gibbons, W. (Eds.), The Geology of Chile. Geol. Soc. Spec. Publ., London, UK, 21–114. ISBN 9781862392199. https://doi.org/10.1144/GOCH.

Cifuentes, I.L., Silver, P.G., 1989. Low-frequency source characteristics of the great 1960 Chilean earthquake. J. Geophys. Res. 94, 643–663, doi:10.1029/JB094iB01p00643.

Clark, M.K., House, M.A., Royden, L.H., Whipple, K.X., Burchfiel, B.C., Zhang, X., Tang, W., 2005. Late Cenozoic uplift of southern Tibet. Geology 33, 525–528. doi:10.1130/G21265.1.

Cristallini, E.O., Ramos, V.A., 2000. Thick-skinned and thin-skinned thrusting in the La Ramada fold and thrust belt: crustal evolution of the High Andes of San Juan, Argentina (32°SL). Tectonophysics 317(3-4), 205–235.

DeMets, C., Gordon, R.G., Argus, D.F., 2010. Geologically current plate motions. Geophys. J. Int. 181(1), 1–80. ISSN 0956540X. https://doi.org/10.1111/j.1365-246X.2009.04491.x.

Dolan, J., Sieh, K., Rockwell, T.K., Yeats, R., Shaw, J., Suppe, J., Huftile, G., Gath, E., 1995. Prospects for larger or more frequent earthquakes in the Los Angeles metropolitan region. Science 267, 199–205. doi:10.1126/science.267.5195.199.

Easton, G., Inzulza, J., Pérez, S., Ejsmentewicz, D., Jiménez, C., 2018. ¿Urbanización fallada? La Falla San Ramón como nuevo escenario de riesgo sísmico y la sostenibilidad de Santiago, Chile. Revista de Urbanismo, Facultad de Arquitectura y Urbanismo, Universidad de Chile, N°38, pp. 1-20.

Estay, J., 2019. Tectónica activa en el borde occidental de la Cordillera Principal de Chile Central (29°-36°S). MSc Thesis (Unpublished), Departamento de Geología, Universidad de Chile, 181 pp.

Estay, J., Pinto., L., Saavedra, C., 2018. Falla Camino del Inca: un registro de ruptura superficial en la Cordillera Principal, Chile central (~32°18'S). Poster, XV Congreso Geológico Chileno, November 18-23, 2018.

Estay, J., Pinto, L.*, Easton, G., De Pascale, G.P., Troncoso, M., Carretier, S., Forman, S.L., 2023. Active thrust tectonics along the western slope of the Central Andes southernmost Pampean flat-slab segment (~33°S, Chile): The Cariño Botado fault system. *Geomorphology* 437, 108801. ISSN 0169-555X. https://doi.org/10.1016/j.geomorph.2023.108801.

Farías, M., Comte, D., Charrier, R., Martinod, J., David, C., Tassara, A., Tapia, F., Fock, A., 2010. Crustal-scale architecture in central Chile based on seismicity and surface geology: Implications for Andean Mountain building. Tectonics 29, TC3006. https://doi.org/10.1029/2009TC002480.

Figueroa, R., Viguier, B., Taucare, M., Yáñez, G., Arancibia, G., Sanhueza, J., Daniele, L., 2021. Deciphering groundwater flow-paths in fault-controlled semiarid mountain front zones (Central Chile). Sci. Total Environ. 771, 145456. ISSN 0048-9697. https://doi.org/10.1016/j.scitotenv.2021.145456.

Gana, P., Wall, R., 1997. Evidencias geocronológicas Ar40/Ar39 y K/Ar de un hiatus Cretácico Superior– Eoceno en Chile Central (33°–33°30'S). Rev. Geol. Chile 24(2), 145–163.

Gutscher, M.A., Sparkman, W., Bijwaard, H., Engdahl, E.R., 2000. Geodynamics of flat subduction: seismicity and tomographic constraints from the Andean margin. Tectonics 19(5), 814–833.

Hanks, T.C., Kanamori, H., 1979, A moment magnitude scale. J. Geophys. Res. 84, 2348–2350, doi:10.1029/ JB084iB05p02348.

Herrera, S., Farías, M., Pinto, L., Yagupsky, D., Guzmán, C., Charrier, R., 2017. Analogue modeling of rotational orogenic wedges: implications for the Neogene structural evolution of the Southern Central Andes (33°-35°S). In: Proceedings, AGU Fall Meeting, 11-15 Dec 2017, New Orleans, United States, T23D-0635.

Hussain, E., Elliott, J.R., Silva, V., Vilar-Vega, M., Kane, D., 2020. Contrasting seismic risk for Santiago, Chile, from near-field and distant earthquake sources. Nat. Hazards Earth Syst. Sc. 20(5), 1533–1555.

Inzulza, J., Gatica, P., Easton, G., Pérez, S., 2021. ¿Diseño urbano resiliente en el piedemonte de Santiago? Contraste de escenarios comunales con riesgo sísmico frente a la Falla San Ramón. Revista Urbano 43, 96–107.

Inzulza, J., Curihuinca, M., Easton, G., Pérez, S., 2022. Revelando el riesgo sísmico en el piedemonte de Santiago, Chile. Análisis multicriterio para la determinación de vulnerabilidad en la Falla San Ramón (FSR). Revista de Geografía Norte Grande 81, 305–330.

Jara, P., Charrier, R., 2014. Nuevos antecedentes estratigráficos y geocronológicos para el Meso–Cenozoico de la Cordillera Principal de Chile entre 32° y 32°30'S. Implicancias estructurales y paleogeográficas. Andean Geol. 41(1), 174–209. http://dx.doi.org/10.5027/andgeoV41n1-a07.

Jordan, T.E., Isacks, B., Ramos, V.A., Allmendinger, R.W., 1983a. Mountain building in the Central Andes. Episodes 1983(3), 20–26.

Jordan, T.E., Allmendinger, R.W., Brewer, J.A., Ramos, V.A., Ando, C.J., 1983b. Andean tectonics related to geometry of subducted Nazca plate. Geol. Soc. Am. Bull. 94, 341–361.

Kanamori, H., 1995. The Kobe (Hyogo-ken Nanbu), Japan, earthquake of January 16, 1995. Seismol. Res. Lett. 66, 6–10. doi: 10.1785/gssrl.66.2.6.

Lossada, A.C., Giambiagi, L., Hoke, G.D., Fitzgerald, P.G., Creixell, C., Murillo, I., Mardonez, D., Velásquez, R., Suriano, J., 2017. Thermochronologic evidence for late Eocene Andean Mountain building at 30°S. Tectonics 36, 2693–2713.

Manea, V.C., Pérez-Gussinyé, M., Manea, M., 2012. Chilean flat slab subduction controlled by overriding plate thickness and trench rollback. Geology 40(1), 35–38.

Martinod, J., Gérault, M., Husson, L., Regard, V., 2020. Widening of the Andes: an interplay between subduction dynamics and crustal wedge tectonics. Earth Sci. Rev. 204, 103170. https://doi.org/10.1016/j.earscirev.2020.103170.

Medina, J., 2018. West Andean Thrust System (WATS) y la caracterización y descripción de la Falla Cariño Botado. Undergraduate Thesis (Unpublished), Departamento de Geología, Universidad de Chile, 69 pp.

Mescua, J.F., Giambiagi, L., Barrionuevo, M., Tassara, A., Mardonez, D., Mazziteli, M. Lossada, A., 2016. Basement composition and basin geometry controls on upper-crustal deformation in the Southern Central Andes (30-36°S). Geol. Mag. 153(5/6) 945–961, Cambridge University Press. https://doi.org/10.1017/S0016756816000364.

Millanao, J., Pinto, L., Cortés, J., Giambiagi, L., Jara, P., 2023. Análisis de la zona de falla Pocuro en el sector Campos de Ahumada: Evidencias de estructuras de transferencia y sus implicancias en la deformación del borde occidental del orógeno Andino (~32°43`S). Actas del XVI Congreso Geológico Chileno, Santiago, Chile, Nov. 26-Dec. 1.

Muñoz-Sáez, C., Pinto, L., Charrier, R., Nalpas, T., 2014. Influence of depositional load on the development of a shortcut fault system during the inversion of an extensional basin: The Eocene-Oligocene Abanico Basin case, central Chile Andes (33°-35°S). Andean Geol. 41(1), 1–28. http://dx.doi.org/10.5027/andgeoV41n1-a01.

Padilla, H., Vergara, M., 1985. Control estructural y alteración tipo campo geotérmico en los intrusivos subvolcánicos Miocénicos del área Cuesta Chacabuco–Baños del Corazón, Chile Central. Rev. Geol. Chile 24, 3–17.

Pardo-Casas, F., Molnar, P., 1987. Relative motion of the Nazca (Farallón) and South American plates since late Cretaceous times. Tectonics 6(3), 233–248.

Pérez, A., Ruiz, J.A., Vargas, G., Rauld, R., Rebolledo, S., Campos, J., 2013. Improving seismotectonics and seismic hazard assessment along the San Ramón fault at the eastern border of Santiago city, Chile. Natural Hazards 71, 243– 274. doi:10.1007/s11069-013-0908-3.

Pérez, C., Pinto, L., Espinoza, M., 2023. Análisis geométrico y cronológico de los sistemas estructurales al norte de los 33°S: Implicancias en la tectónica andina al norte y sur de la depresión Los Andes-San Felipe. In: Proceedings XVI Congreso Geológico Chileno, Santiago, Chile, Nov. 26-Dec. 1.

Ritz, J.F., Nazari, H., Balescu, S., Lamothe, M., Salamati, R., Ghassemi, A., Shafei, A., Ghorashi, M., Saidi, A., 2012. Paleoearthquakes of the past 30,000 years along the North Tehran fault (Iran). J. Geophys. Res. 117, B06305. doi:10.1029/2012JB009147.

Rivano, S., 1996. Geología de las Hojas Quillota y Portillo, Región de Valparaíso. Servicio Nacional de Geología y Minería, Carta Geológica de Chile, Nº 73 (Unpublished), 232 pp. Santiago, Chile.

Rivano, S., Sepúlveda, P., Boric, R., Espiñeira, D., 1993. Hojas Quillota y Portillo, V Región. Servicio Nacional de Geología y Minería, Carta Geológica de Chile, Map 73, scale 1:250,000.

Rodríguez, M.P., Charrier, R., Brichau, S., Carretier, S., Farías, M., de Parseval, P., Ketcham, R.A., 2018. Latitudinal and Longitudinal Patterns of Exhumation in the Andes of North-Central Chile. Tectonics 37. https://doi.org/10.1029/2018TC004997.

Rubin, C., Lindvall, S., Rockwell, T.K., 1998. Evidence for large earthquakes in metropolitan Los Angeles. Science 281, 398–402. doi:10.1126/science.281.5375.398.

Salomon, E., Schmidt, S., Hetzel, R., Mingorance, F., Hampel, A., 2013. Repeated folding during late Holocene earthquakes on the La Cal thrust fault near Mendoza city (Argentina). Bull. Seismol. Soc. Am. 103, 936–949. doi:10.1785/0120110335.

Sernageomin, 2003. Mapa geológico de Chile, versión digital, Servicio Nacional de Geología y Minería, 1 Map, scale 1:1,000,000.

Sobolev, S., Babeyko, A., 2005. What drives orogeny in the Andes? Geology 33(8), 617–620. https://doi.org/10.1130/G21557AR.1.

Tapia-Canelo, C., 1944. Los Andes históricas relaciones. Archivo de Literatura Oral y Tradiciones Populares. Disponible en Biblioteca Nacional Digital de Chile https://www.bibliotecanacionaldigital.gob.cl/bnd/627/w3-article-346710.html.

Taucare, M., Roquer, T., Heuser, G., Pérez-Estay, N., Arancibia, G., Yáñez, G., Viguier, B., Figueroa, R., Morata, D., Daniele, L., 2022. Selective reactivation of inherited fault zones driven by stress field changes: Insights from structural and paleostress analysis

of the Pocuro Fault Zone, Southern Central Andes (32.8°S). J. South Am. Earth Sci. 118, 103914. ISSN 0895-9811. https://doi.org/10.1016/j.jsames.2022.103914.

Troncoso, M., 2014. Evidencia geomorfológica de neotectónica en el borde oriental de la Depresión de Los Andes-San Felipe, Provincia de Los Andes, Región de Valparaíso. MSc Thesis (Unpublished), Departamento de Geología, Universidad de Chile, 107 pp.

Urrejola-Sanhueza, J.T., 2022. Análisis estructural mediante magnetotelúrica del Sistema de fallas Pocuro entre el Estero San Francisco y el Río Aconcagua, V Región. Undergraduate Thesis (Unpublished), Departamento de Geología, Universidad de Chile, 104 pp.

Vargas, G., Klinger, Y., Rockwell, T.K., Forman, S.L., Rebolledo, S., Baize, S., Lacassin, R., Armijo, R., 2014. Probing large intraplate earthquakes at the west flank of the Andes. Geology 42(12), 1083–1086. https://doi.org/10.1130/G35741.1.

Vigny, C., Rudloff, A., Ruegg, J.-C., Madariaga, R., Campos, J., Álvarez, M., 2009. Upper plate deformation measured by GPS in the Coquimbo Gap, Chile. Phys. Earth Planet. Inter. 175(1-2), 86–95.

Xu, X., Wen, X., Yu, G., Chen, G., Klinger, Y., Hubbard, J., Shaw, J., 2009. Coseismic reverse- and oblique-slip surface faulting generated by the 2008 Mw 7.9 Wenshuan earthquake, China. Geology 37, 515–518, doi:10.1130/G25462A.1.

Acknowledgments: This study was mainly supported by the Fondecyt Project 1200871 (L. Pinto) and secondary by Fondecyt Project 11160038 (G. de Pascale) and the Chilean National Emergency Office of the Ministry of the Interior and Public Security (ONEMI) under resolution No. 41, 20 June 2016 (Seismic monitoring and seismogenic potential of the San Ramón Fault). We also appreciate grants from the Fondecyt Project 1090165 (L. Pinto), from which the first observations of the Cariño Botado fault were made. G. de Pascale is supported by the Earth Science Institute of the University of Iceland's start-up fund and the University of Iceland Research Fund. We want to thank a lot of people for their invaluable help with this research: the Cariño Botado community for their hospitality to working at the study region, in particular to C. Quiroga ('la abuelita del cerro') and C. Henríquez, who always kindly opened their homes to visit the outcrops in the Llano Norte and the San Francisco Creek; R. Charrier, M.P. Rodríguez, P. Jara, R. Abrahami and R. Rauld for their valuable discussion on the field; V. Flores and M. San Juan for their revisions of sedimentology and stratigraphy of alluvial fan deposits; J. Vargas for the separation of zircons; V. Valencia for U-Pb geochronology of detrital zircons; and P. Brunetti, A. Said, J. Medina, and C. Troncoso, for their help in taking samples and structural and geomorphological data. We appreciate the revision of A. Jackson-Gain for improving the English on the first version of this article.